

On the investigation of voltage controlled oscillator phase noise for IoT applications

F. Haddad, W. Rahajandraibe, and I. Ghorbel

Aix-Marseille University, IM2NP UMR CNRS 7334, Technopole château Gombert, 13013 Marseille, France

Abstract. Voltage controlled oscillator (VCO) is one of the key elements in radio frequency (RF) transceivers. A VCO working at 2.4 GHz and designed in CMOS technology is presented. It is suitable for low-cost and low-noise applications using wireless standards such as ZigBee, Bluetooth, Wi-Fi and WPAN (Wireless Personal Area Network). The noise characteristics of this RF VCO are investigated. Noise measurements, especially, phase noise are achieved under different environmental conditions.

1. Introduction

The last few years have seen a dramatic rise in Internet of Things (IoT) devices and connected products such as wireless sensors, home automation systems, smart meters, wearable, etc. [1]. Gartner estimates that 4 billion connected things will be in use in the consumer sector in 2016, and will reach 13.5 billion in 2020 [2]. The network topology of IoT systems consists of nodes that collect and transmit a limited amount of data to a central controller. Figure 1 presents the architecture of a typical IoT sensor node. It is comprised of a processor unit or a microcontroller (MCU) that processes data and runs software stacks interfaced to a wireless device for connectivity.

Sensor nodes should be portable and able to work under batteries or even able to harvest ambient energy for several years. The main challenge consists in minimizing power consumption and extending wireless connectivity range. To this end, several low-power and low-cost narrow-band standards, such as IEEE 802.15.4 (LR-WPAN) [3] and Bluetooth Low Energy [4] have emerged.

The wireless transceiver is an important part of IoT systems. It achieves transmission (TX) and reception (RX) of the data using radio frequency (RF) connectivity (cf. Fig. 1). The 2.4 GHz frequency is a good choice to serve the transceiver designer needs, given the high profile of this 2.4 GHz ISM (industrial, scientific and medical) band with many existing wireless standards such as ZigBee, Bluetooth, Wi-Fi and LR-WPAN.

The transceiver must be low power, low cost, reliable and able to operate under varied environmental conditions regardless of RF interference and noise. The RF front-end building blocks must meet drastic power constraints. In fact, the power consumption depends on the required signal-to-noise ratio (SNR) to transmit the data (commonly expressed as bit-error-rate BER, in digital transmission). In order to optimize the power consumption, one possibility consists in quantifying as precisely as possible the circuit noise floor. Knowing that allows to optimize significantly the over-power consumption of the building blocks.

At the heart of transceivers is an RF voltage controlled oscillator (VCO), as shown in Fig. 2. It generates signals that can be used for frequency synthesis and clock generation for

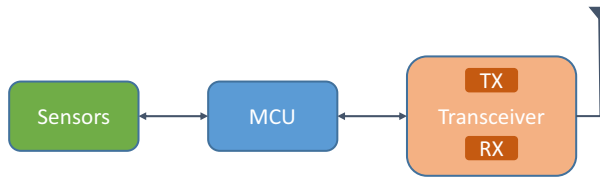


Figure 1. IoT sensor node topology.

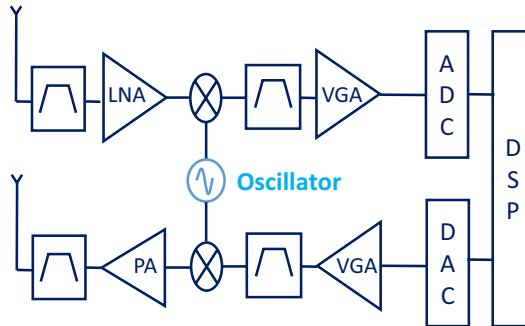


Figure 2. Generic wireless transceiver architecture.

example. VCOs can be divided into two main categories: LC-VCO and ring-VCO. Ring oscillators are characterized by a wide tuning range and low area occupation, while LC oscillators have better phase noise compared to ring oscillators due to the high Q inductors.

In this paper, a low-cost RF VCO is designed and implemented in CMOS technology. Noise characteristics, especially in terms of phase noise, are investigated and measured under different environmental conditions. The rest of the paper is organized as follows. In section II, the VCO topology is introduced and its phase noise analysis in noisy environment is presented. In section III, noise measurements are presented and analyzed. Section IV draws some conclusions.

2. CMOS VCO design

Research on wireless communications has drawn a trend towards design of highly integrated, low-cost and low-power circuits and systems. To achieve these design goals, different topologies of transceivers have been proposed in the literature [5]. Heterodyne transceivers have been widely used in second generation (2G) of wireless telephone technology thanks to its high performances in terms of selectivity and sensitivity. Intermediate frequency (IF) is used for the down-conversion procedure and leads to aliasing of the image frequency inside the useful signal band. The homodyne, architecture uses direct conversion method in order to overcome the image and integration problems leading to low cost solution. However, it achieves much lower performances than heterodyne receiver. “Low-IF” receiver allows combining the advantages of both architectures, i.e. high performances and fully integrated devices. Figure 2 shows a typical low-IF transceiver architecture. It contains many blocks such as low noise amplifier (LNA), filters, voltage gain amplifier (VGA), power amplifier (PA), mixer, converters (ADC, DAC), etc. It can be seen that the oscillator is an essential block in both sides (RX and TX) of the transceiver.

There are many VCO structures proposed in literature. The structure using RC has some restrictions such as the large layout area, noise performance, and small tuning range. LC

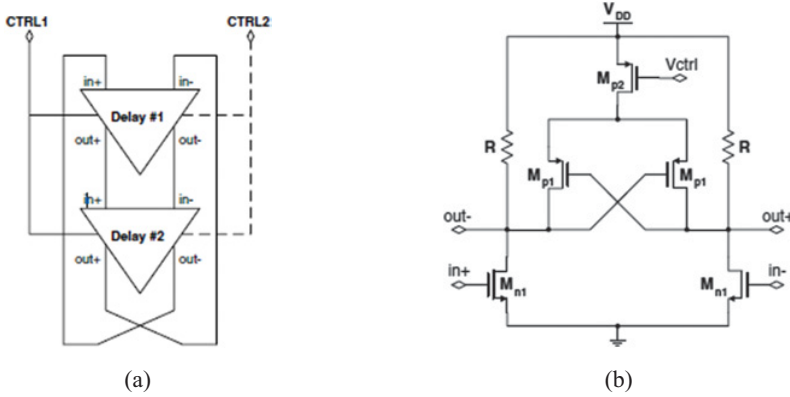


Figure 3. CMOS VCO: (a) schematic with two delay stages and (b) implementation of one cell.

structure based oscillators allow very low phase noise and good spectral purity of the output frequency, but suffer of low tuning range and the difficulty to integrate the inductor part. Ring oscillators have become essential building block in VCO's [6] as their achievable performance can fit number of telecommunication standards like Bluetooth or IEEE 802.15.4 WPAN applications with relatively low area occupation and low consumption. The schematic of the well-known ring oscillator is illustrated in Fig. 3a. At first, we do not consider the dashed line corresponding to CTRL2.

A VCO, initially proposed in [7] is used to implement the oscillator function. The schematic principle of the VCO, given in Fig. 3b, uses NMOS differential pair (M_{n1}) as input stage.

It is connected to an active load formed by a cross coupled PMOS transistor (M_{p1}) which plays the role of a negative resistance, itself connected to the control transistor (M_{p2}). They are put in parallel with polysilicon resistors which are directly connected to the supply voltage (V_{DD}). If the gate voltage of M_{p2} rises, the injected current decreases and reduces in the same way the value of the negative resistance. Thus, the total load resistance of the pair increases and leads to a reduction of the oscillation frequency. At first, we do not consider the dashed line corresponding to CTRL2 (used to control the frequency temperature drift). The centre frequency of the VCO is controlled by the voltage CTRL1, as illustrated in the schematic of the implemented circuit in Fig. 4.

Only two cross-connected delay cells are used to obtain oscillations. That permits to keep power consumption low, low silicon area and reduced phase noise. In order to simplify the expression, let us note $R_T = r_{dsn1} // r_{dsp1} // R$ and $C_T = C_{dbn1} + C_{dsp1} + C_{dbp1} + C_{gdn1} + C_L$, with C_L as the load capacitance. Thus, the differential transfer function can be deduced as

$$A(s) = \frac{V_{out}}{V_{in}} = \frac{g_{mn1} R_T \left(1 + s \frac{C_{gdn1}}{g_{mn1}}\right)}{\left(1 - R_T g_{mp1}\right) \left(1 + s \frac{R_T C_T}{1 - R_T g_{mp1}}\right)} \quad (1)$$

from which, f_0 can be deduced according to Barkhausen criteria, such as $|A(j\omega_0)| = 1$, and is expressed as

$$f_0 = \frac{1}{2\pi} \sqrt{\frac{(g_{mn1})^2 - \left(\frac{1}{R} - g_{mp1}\right)^2}{C_T^2 - C_{gdn1}^2}} \quad (2)$$

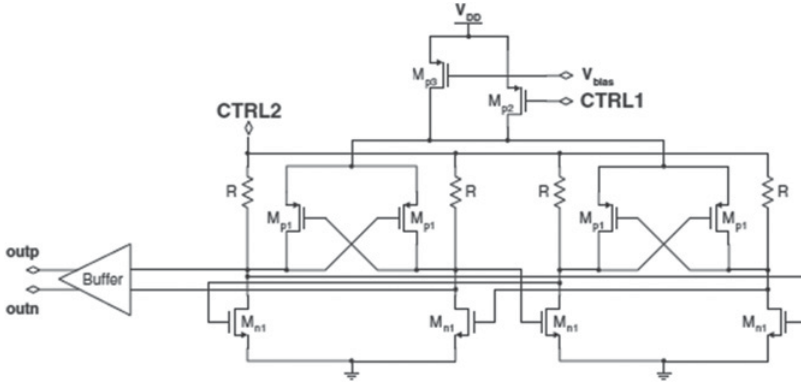


Figure 4. Schematic of the implemented VCO.

Simulations have been done using *Cadence*[®] tool and *Spectre-RF* simulator. A total frequency range of 453 MHz around 2.45 GHz is obtained for a control voltage extending from 0 to 2.5V with a phase noise of -102 dBc/Hz at 1 MHz offset.

3. Phase noise theory

The phase noise is considered as one of the most important factors which limit the quality of communication systems. In most applications, it is necessary that the phase noise of oscillators be kept at sufficiently low level. For an ideal oscillator operating at f_0 , the spectrum assumes the shape of an impulse. Nevertheless, practical oscillators, like any other RF components, are non-ideal, always have intrinsic noise that modulates the signal and causes fluctuations in its amplitude and phase, leading to imperfect spectral purity. The oscillator's frequency spectrum exhibits sidebands around the carrier f_0 as shown in Fig. 5. As can be seen, the phase noise effectively causes the frequency of the oscillator fluctuate around f_0 . Therefore, when an oscillator is used in systems, its signal contains not only the real RF signal but also unwanted RF noise signals causing degradation in the performance of corresponding systems. For instance, an oscillator with high phase noise produces large unwanted sideband noise signals, possibly causing radiation of unwanted signals for transmitters, unwanted mixing products in receivers, degradation of the signal-to-noise ratio (SNR) of receivers, etc.

We consider a general signal spectrum of oscillators as shown in Fig. 5. The phase noise at frequency f_m offset from the carrier's frequency f_0 is defined as the ratio of a single-sideband noise power (P_{noise}) in a 1-Hz bandwidth at f_m to the carrier's total power (P_{signal}) [5, 8].

The Hajimiri and Lee model [9] is generally used to calculate the theoretical phase noise of oscillators. For a ring oscillator, the pulse sensitivity root mean square function, noted Γ_{rms} , can be calculated with the following expression:

$$\Gamma_{\text{rms}} = \sqrt{\frac{2\pi^2}{3\alpha^3}} \frac{1}{N^{1.5}} \quad (3)$$

where N is the cell number that composes the VCO, α is a proportionality constant depending to the used structure. In our case $\alpha = 0.9$, so that $\Gamma_{\text{rms}} = 3/N^{1.5}$. The phase noise is then

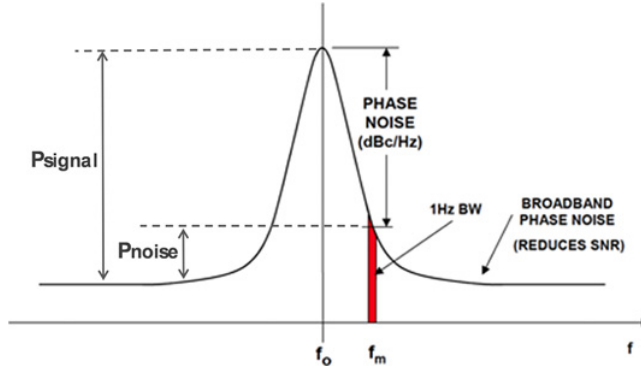


Figure 5. Oscillator's frequency spectrum showing the effect of phase noise on frequency.

calculated as

$$L(f_m) = \frac{\Gamma_{rms}^2}{8\pi^2 f_m^2} \frac{\left(\overline{i_n^2}/\Delta f\right)_{total}}{q_{max}^2} \cdot 2N. \quad (4)$$

The spectral density of noise current sources inside the circuit can be written as

$$\left(\frac{\overline{i_n^2}}{\Delta f^2}\right)_{MOS} = 4kT\gamma g_m, \quad \left(\frac{\overline{i_n^2}}{\Delta f^2}\right)_R = \frac{4kT}{R} \quad (5)$$

where γ is the channel length related coefficient of the used transistor, that, for short channel MOS in the saturation region is typically equal to 2, k is the Boltzmann constant, T is the absolute temperature, and g_m is the transconductance. We can calculate the total noise spectral density by summing that of each element such as

$$\left(\frac{\overline{i_n^2}}{\Delta f^2}\right)_{total} = \left(\frac{\overline{i_n^2}}{\Delta f^2}\right)_{n1} + \left(\frac{\overline{i_n^2}}{\Delta f^2}\right)_{p1} + \left(\frac{\overline{i_n^2}}{\Delta f^2}\right)_R + \frac{1}{4} \left(\left(\frac{\overline{i_n^2}}{\Delta f^2}\right)_{p2} + \left(\frac{\overline{i_n^2}}{\Delta f^2}\right)_{p3} \right). \quad (6)$$

Thus a theoretical phase noise of -101 dBc/Hz is obtained at 1 MHz offset from the carrier. This value is very closed to the simulation result of -102 dBc/Hz.

4. Noise measurements

A two-stage ring oscillator working around 2.45 GHz has been fabricated in a 0.28 CMOS technology. The photograph of the circuit test chip is depicted in Fig. 6a. The VCO occupies a low area of $110 \mu\text{m} \times 110 \mu\text{m}$.

The measurement setup of on-chip RF circuits is very complex, especially if noise requirements are stringent (case of RF oscillators). The used probe station is shown in Fig. 6b. First, DC and RF probing are positioned into the PADs on the wafer. Then, they are connected with RF cables to the spectrum analyzer. Special attention must be paid to the probing 50Ω calibration to meet measuring instruments needs. Besides, resolution bandwidth (RBW) of the spectrum analyzer should be calibrated, since it can be important versus the noise bandwidth. Noise floor of the setup measurement need to be calibrated as well.

Measurements were performed at nominal operating conditions: room temperature, supply voltage of 2.5V and a control voltage of 1V. In these conditions, noise and

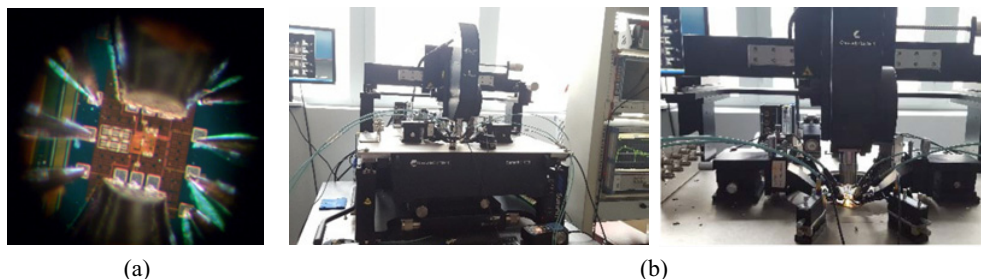


Figure 6. Photograph of the circuit test chip (a) on-chip measurement setup.

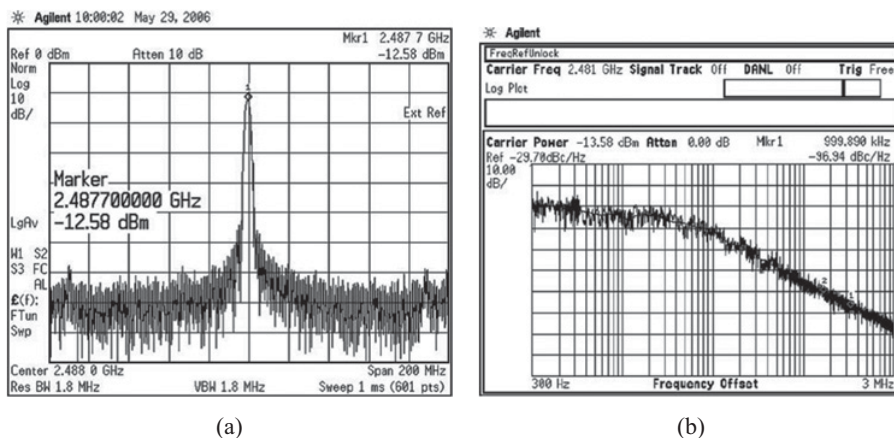


Figure 7. VCO measured (a) frequency spectrum and (b) phase noise profile.

interferences are all around the measuring station, and will certainly degrade the noise floor characteristic of the VCO.

In one side, the output frequency spectrum measured from one circuit sample is depicted in Fig. 7a. It exhibits a signal power of -12.58dBm at 2.48GHz . In the other side, the phase noise of the total circuit profile is depicted in Fig. 7b and shows a -96.9dBc/Hz at 1MHz offset from the carrier. A slight degradation of the phase noise is then observed during the measurement under noisy environment. RF circuit characterization such as noise measurement is usually done with anechoic chamber. Nevertheless, the calibration of the chamber requires high cost equipment like vector network analyzers (VNA) and “Termination-VSWR” method to measure the reflectivity of an absorber wall in an anechoic chamber. Moreover it requires sophisticated mathematical treatments to be made on the measured signals such as Fourier transform, allowing calculation of echoes in the time domain, filtering and removal of unwanted echoes (time-gating capability), and returning back to the frequency domain with an improved measurement accuracy.

LSSB facilities with well-known noise characteristics and calibrated environment are a good opportunity to perform VCO phase noise measurement as a future work. One must point out the VCO’s intrinsic noise floor characterization in order to investigate the phase noise profiles in different environments.

5. Conclusion

VCO's are an integral part of building block for *IoT* wireless transceivers. It was given in this paper that random fluctuations in the output frequency of VCO's, expressed in phase noise, have a direct impact on the timing accuracy where phase alignment is required and on the signal-to-noise ratio where frequency translation is performed. Then, phase noise in RF oscillators has been investigated. A 2.45 GHz multi-controlled ring oscillator has been implemented with full CMOS process.

Measurement setup and obtained results in a nominal condition (a room environment with noise and interferences around the measuring station) have been presented. It was noted that noise floor needs to be performed in low-noise environment. Thus, VCO noise characterization will be performed in the near future in LSBB facilities.

References

- [1] M. Lieshout, et al., "Converging Applications enabling the Information Society", Report Community research, *Future Technologies Division of VDI Technologiezentrum GmbH* (2010).
- [2] Gartner, "IoT rapid prototyping to proof your business case", Gartner Symposium/ITxpo, Barcelona, Spain (2015).
- [3] IEEE Standard for Local and Metropolitan Area Network – Part 15.4: Low Rate Wireless Personal Area Network (LR-WPAN), IEEE Standard 802.15.4-2011 (2011).
- [4] Bluetooth Specification, Core package v4.0, Bluetooth-SIG, Kirkland, WA, USA (2010).
- [5] B. Razavi, *RF Microelectronics*, Prentice Hall 2nd Edition (2011).
- [6] A. Hajimiri, S. Lymtyrakis, and T.H. Lee, "Jitter and phase noise in ring oscillator." *IEEE Journal of Solid-State Circuits*, **34**, pp. 790–804 (1999).
- [7] W. Rahajandraibe, et al., "Temperature Compensated 2.45 GHz Ring Oscillator with Double Frequency Control," in Proc of IEEE Radio Frequency Integrated Circuits Symposium (RFIC'07), Honolulu, Hawaii, pp. 409–412 (2007).
- [8] C. Nguyen, *Radio frequency integrated circuit engineering*, Wiley series in Microwave and optical engineering, John Wiley & Sons (2015).
- [9] A. Hajimiri and T.H. Lee, "A general theory of phase noise in electrical oscillators." *IEEE Journal of Solid-State Circuits*, **33**, no. 2, pp. 177–194 (1998).